Low Speed Nano/Micro/Meso-Scale Rarefied Flows Driven by Temperature and Pressure Gradients

E.P. Muntz,
A.A. Alexeenko*, S.F. Gimelshein*, A.D. Ketsdever**, Y.-L. Han*,
M.P.Young**, J.H. Park*, C. Ngalande* , N.P. Selden*, R.H.Lee*

** University of Southern California, Department of Aerospace and Mechanical Engineering*
Los Angeles, CA 90089-1191
*** United States Air Force Research Laboratory, United States Air Force Research Laboratory*
Edwards Air Force Base, CA 93524, USA

Abstract. Gas flows in nano/micro-scale channels are of considerable practical as well as scientific interest. The present discussion is guided by experience gained during investigations at USC of three technologies; all involving the use of gas flows in both relatively long and short channels with characteristic cross-sectional dimensions from millimeters to nanometers. One technology is a meso-scale, continuous trace-gas pre-concentrator, for portable detection of fractional trace-gas concentrations down to 1E-12. Flow channels in the pre-concentrator, which range in characteristic lateral dimensions from several tens of micrometers to below one nanometer, can be driven by either relatively modest pressure and/or temperature differences. Another technology is a micro/meso-scale solid state compressor or vacuum pump, now relatively well known as the Knudsen Compressor. It has no moving parts and is driven by thermal creep flow, which in one version is generated by applying longitudinal temperature gradients along the walls of the flow channels. The channels have cross-sectional dimensions varying from hundreds of micrometers to tens of nanometers. Both of these technologies generally operate at around atmospheric pressure or below, resulting in flow conditions that are predominantly in the rarefied and transitional flow regimes. A third technology is the use of thermal creep, or more generally temperature gradient (thermal stress and creep) driven flows, that generate 'radiometric' forces for micro-scale actuators, and perhaps nano/micro/macro-scale actuators. The nano/micro/macro-scale actuators are envisioned as a macro-scale assemblage of large numbers of component nano/micro-scale actuators. The predominant characteristics of thermal creep and thermal stress flows are; relatively low flow speeds, and a requirement for both Knudsen and transitional regime Knudsen numbers in order to provide suitable actuator force levels.

Keywords: Thermal creep, thermal stress, radiometer, Knudsen Compressor, trace gas pre-concentration.
PACS: 47.45-n

INTRODUCTION

An important consideration, for describing and understanding flows in nano/micro-scale channels and radiometric-force-actuators (RFA's),[1,2] is the vastly magnified role of the surfaces of the flow channels or actuators compared to geometrically similar macro-scale flows with the same Knudsen number.[3] The surface topology, as well as the interaction of gas molecules with the molecular lattices that form the surfaces, can have important influences on a flow's characteristics. Also, for most of the range of flow cross-sectional sizes under consideration, the quantity of adsorbed gas on the surfaces can easily be equal to or larger than the amount of gas outside of the influence of the surfaces' potential wells. The development of flow based nano/micro-systems would be significantly simplified if accurate and time-effective numerical modeling were available, particularly in complex geometric situations where high-resolution experimental flow diagnostics is limited, difficult to apply, or impossible. Gas flows in trace-gas pre-concentrators, Knudsen Compressors, and RFA's, are frequently in significant non-equilibrium because of rarefaction effects. Consequently the constitutive relations for the stress tensor and the heat flux vector, in terms of macroscopic parameters (bulk velocity, density, temperature) that appear

in the Navier-Stokes equations, break down. It follows that conventional CFD modeling approaches become unattractive, particularly when difficult wall boundary conditions are anticipated. The modeling should be based on microscopic, kinetic descriptions.

The use of two kinetic approaches will be discussed, with directly comparable examples of their applications to flows that are characteristic for each of the three nano/micro/macro-scale gas flow based technologies mentioned previously. The currently accepted gold standard kinetic approach is the direct simulation Monte Carlo (DSMC) method.[4,5] The DSMC method has proven to be a powerful and validated numerical tool for modeling high-speed, rarefied gas flows.[6] However, applications of this stochastic kinetic approach for low speed gas flow systems is difficult, due to significant computational costs (time) resulting from inherent statistical scatter. It also becomes increasingly computationally costly as the flow Knudsen number decreases towards the continuum flow regime. The second kinetic approach is to obtain deterministic solutions, by applying a discrete ordinate method to the ellipsoidal-statistical (ES) model kinetic equation that provides realistic Prandtl numbers.[7] The primary advantage of this modeling technique is its relatively high computational efficiency compared to the DSMC method, coupled with excellent agreement in predicted, detailed flow properties between the two approaches for both temperature and pressure gradient driven flows. Several examples of the use of both of these techniques to support the interpretation of experimental results have been presented.[7]

The 19th RGD Conference, held at Oxford University during July 1994, marked the revival of Crookes' radiometer as a subject of technical interest. Papers by Wadsworth et al,[8] Pham-Van-Diep et al,[9] Ota and Katawa,[10] Soga et al,[11] and Aoki et al,[12] applied Bird's DSMC technique[4] to the study of selected low speed, thermal stress and thermal creep flows that could be applicable to RFA's. Since that time there have been active experimental, theoretical, and computational developments relating to RFA's, primarily in Japan and the USA. Knudsen Compressors, which were introduced at the Oxford meeting by Pham-Van-Diep et al,[13] have been studied in several forms at the University of Southern California[14,15,16] and at Kyoto University,[17,18,19,20] including one joint paper. [2]

Traditionally, the initial period of interest relating to radiometric forces is considered to have begun in 1873, with the exhibit by W. Crookes of a radiometer at a soirée of the Royal Society of London.[21] From that time up until the 1930's there was an enthusiastic exchange of opinion about the cause of the radiometer effect. Among those contributing to these investigations were; O. Reynolds,[22] J. C. Maxwell,[23] M. Knudsen,[24,25] A. Einstein,[26] H. Marsh, E. Condon, L. Loeb,[27] H. Marsh,[28] G. Hettner,[29] and E. Brueche and W. Littwin.[30] The summaries of this work presented by L. Loeb,[31] E. H. Kennard,[32] and S. Dushman[33] are a convenient review of important studies from 1873 to the late 1930's. More recently there has been a steady effort from a broad community located in Asia, Europe, North America, and Australia, involved in developing analytical and numerical techniques for studying low speed, non-isothermal, rarefied flows. M. Kogan and his colleagues in Russia have studied slow non-isothermal flows[34,35,36] in a gas where ($\Delta T/T$)~1 (SNIFs in their terminology). Contributions from Y. Sone and his colleagues at Kyoto University addressed slow rarefied flows for both high[37] and low[38] Knudsen numbers. A very recent monograph by C. Cercignani, addresses the subject of slow rarefied flow applied to micro-electromechanical systems[39]. Finally, the development by G. Bird[40,4] of the DSMC technique coupled with suggestions by his many disciples has provided, as of the 1990's, an effective although somewhat time consuming tool for studying slow, non-isothermal rarefied flow problems at not extremely small Knudsen numbers.

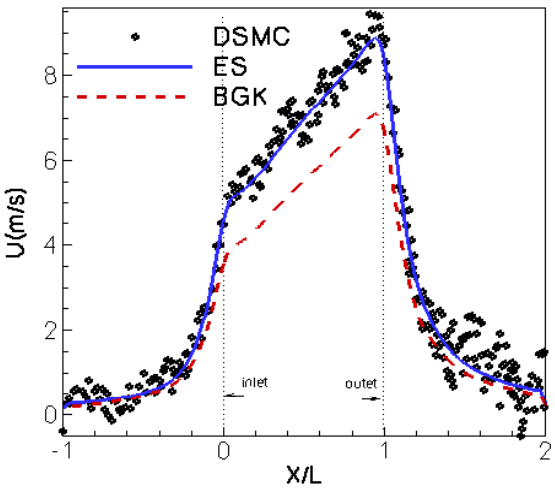

Figure 1: X-component of Velocity along the Channel Centerline Obtained by DSMC, ES and BGK Models for a Temperature Gradient Driven Flow in a 2-D Channel[44]

The DSMC technique is invaluable in helping to sort out questions raised by experimental results in areas discussed later in the paper. However it does not have as fast a turnaround time in this role as one might hope. Because of this, the USC group has been looking at the possibility of applying the Elliptical-Statistical (ES) model of the Boltzmann equation to the types of flows that appear in our experiments. This development has been pursued primarily by A. Alexeenko in collaboration with S. Gimelshein and others.[7,41,42,43] The ES model has resulted in several recent publications. It has been very successful in providing accurate results as established by comparison to the same calculations by the DSMC technique. At the same time, it typically results in

significantly greater than a 10 times reduction in computation time. Details of this research are presented in the references mentioned above. An example of a typical comparison is presented in Fig. 1 for a temperature gradient driven flow.[44]

RADIOMETRIC FORCE ACTUATORS (RFA'S)

Enclosed RFA's

In 1996 Wadsworth et al[45] published the results of a computational investigation, using the DSMC method, for an enclosed micro-scale radiometric force actuator (ERFA). A schematic cross-sectional view of the actuator is shown in Fig 2, with dimensions used in the study reviewed in Table I. The force surfaces (1,2,3,4) that define a typical radiometric enclosure are indicated in Fig.2. They were assumed to be held at temperatures $T_1=T_2=T_3=$ 300K, and T_4=600K. Because of concerns about maintaining large temperature differences in micro-scale devices, a transient heating variant for surface 4 was integrated with the vane configuration illustrated in the lower half of Fig. 2 (in an actual actuator both sides of the actuator would have to be similar in order to balance significant forces that occur normal to the x-direction). In the transient variant every vane is a distance H thick in the x direction. Changing the angle θ was studied but for the results discussed here $\theta = 45^o$. A condensed version of the results are presented in Table II. Detailed discussions for the thick wall transient heating option is discussed in Ref 45. It is clear from Table II that the constant heating option produces much higher forces, but the difficulty in maintaining relatively larger temperature difference in micrometer sized enclosures likely dictates that some form of transient temperature difference would have to be adopted. A study of "Thermal Transpiration at Microscale", using transient heating of a cantilever, recently has been reported by Passian et al. [46] This study has made in part made use of semi-enclosed RFA's. Very recently, a macro-scale ERFA has been built and tested by Park.[47] The vanes were mounted in a 15 cm. diameter, 25 cm. long cylindrical array, corresponding to the illustration for thin vanes in Fig. 2. In this case the analog to surface 3 was cooled by liquid nitrogen and surface 1 was heated by a resistive heater. The vanes were 2mm thick aluminum, which maintained a constant temperature roughly half way between the hot and cold surface temperatures. The pressures in the test environment were 100–400 mTorr. The torque generated by the vanes was measured and compared to results predicted from DSMC simulations. Knudsen numbers, temperatures and pressures observed during the experiments were used in the calculations. A typical example of predicted and experimental torques, normalized by the pressure for each experiment or simulation, is presented in Fig 3. The agreement is quite reasonable considering the depressed zero of the torque/Pressure axis, and the difficulty of the experiments.

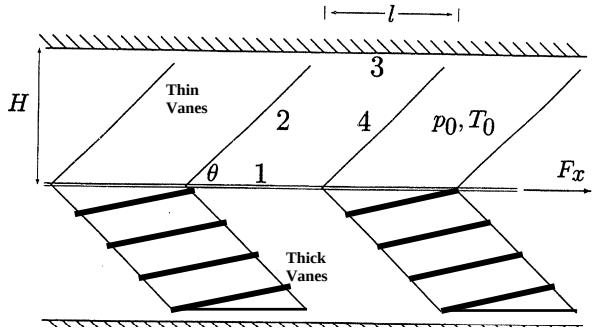

Figure 2 Force Surfaces of a ERFA Actuator[45]

Quantity	Unit	H= 10μm	H = 1μm	H=0.1 μm
Vane Width	μm	100	100	100
Actuator Length	μm	100	100	100
Number of Thin Vanes (slider 0.5 length of actuator)	--	5	50	500
Number of Thick Vanes (transient heating option)	--	2.5	25	250
Knudsen Number Based on H	--	7E-3	7E-2	7E-1

Table I Geometry of Two Model ERFA's. Wadworth's DSMC Calculations[45]

Quantity	Unit	H= 10μm	H = 1μm	H=0.1 μm
Radiometric Force Per Unit Cross-Sectional Area, Thick Vanes (transient heating)	N/m^2	1.5E2	6.5E2	1.7E2
Radiometric Force Per Unit Cross-Sectional Area of Actuator, Thin Vanes (constant heating)	N/m^2	3.0E2	1.3E2	3.4E2

Table II Summary of Results from Calculations for Two ERFA's[45]

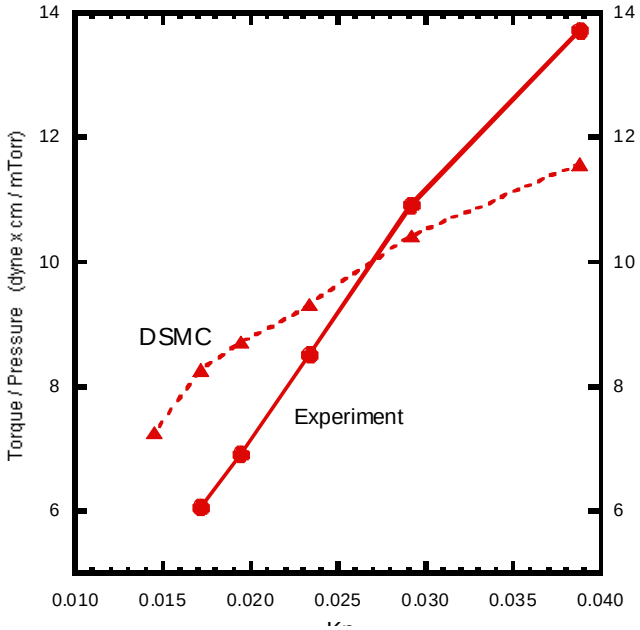

Figure 3 Comparison of DSMC Predictions and Experiment by Park. Diffuse Reflections Were Assumed for the Prediction[47]

Open RFA's

The alternative to ERFA's is the open RFA or ORFA. Crookes radiometer was an ERFA due to the close proximity of the glass bulb in which the vanes rotated. There have been a number of recent discussions relating to the use of radiometric forces to maintain vehicles at high altitudes. This is an open radiometric force phenomena since, unlike Crookes radiometer, the thermal creep flow field has no boundaries. One such approach[48], proposes a ground based microwave beam to support a radiometric force vehicle at an altitude of about 70 km. The microwave beam creates temperature differences in carbon fiber sails attached to a payload. The fibers are about one local mean free path in diameter. The fibers are also separated from each other by a distance of about one local mean free path. This approach has been based on an idea, proposed by Einstein,[26] that a significant fraction of the force generated by an open radiometer at low Kn is provided by a one mean free path wide strip at the edge of the radiometer vane. This suggestion has never been convincingly demonstrated experimentally. Furthermore, to increase the effect, it has been suggested that a large number of small flow channels, connecting the hot and cold surfaces, be embedded in a large radiometer vane. Each channel would be about one mean free path in cross-sectional characteristic size,. This strategy of using a large number of partly enclosed RFA's (PERFA) in principle can provide a significantly increased edge area. Also, there would be an additional thrust due to the thermal creep pumping of gas from cold to hot through the channels. If all of the newly made edge area contributed according to Einstein's hypothesis, the increased edge effect would provide a much greater force increase than the thrust originating from the flow through the channels.

The USC group has been looking at this issue both experimentally (N. Selden, A. Ketsdever) and using DSMC simulations (S. Gimelshein, C. Ngalande). From our present experiments and calculations, there is no indication that Einstein's hypothesis can be extended to densly packed mean free path scale elements in a continuum vane. The results of this USC study should be available by the end of 2007.

KNUDSEN COMPRESSORS AND RADIOMETRIC PHENOMENA

During the investigation of low-pressure Knudsen Compressor performance, [16,49] rarefaction effects other than thermal creep flows were observed. The temperature gradient imposed on the Knudsen Compressor membrane's surface has induced internal flow circulation in the connector section.[50] The flow circulation is similar to what was observed by Wadsworth in his study of Crookes' radiometer.[8] The original Knudsen Compressor performance model employed flow coefficients, calculated from a linearization of the Boltzmann equation, that could not accurately predict this complex flow situation.

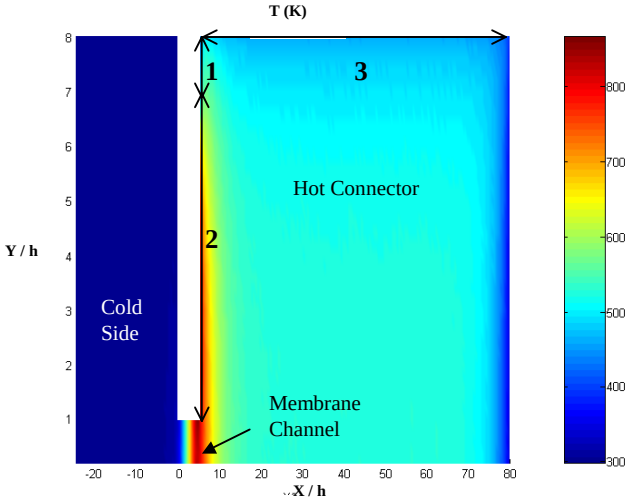

Figure 4 Gas Temperature Map of the Knudsen Compressor from a DSMC Simulation

Using the DSMC simulation technique, thermal creep flows through a short (length/height = 5, h =height of the membrane channel) 2-D channel were studied.[51] One particular temperature profile of the simulation domain is shown in Fig 4. This particular case was designed to mimic the experimental single stage design,[16] which had a discontinuous temperature profile. As shown in Fig. 4, section 1 and section 2 of the vertical wall were kept respectively at a constant cold temperature (T_L) and a constant hot temperature (T_H). The horizontal wall of the hot chamber (section 3) was set to be a constant cold temperature (T_L). Due to the temperature profile along the walls, flow circulations were induced near the outlet of the membrane channel as shown in Fig. 5. The pressure increase through a Knudsen Compressor stage is an important performance indicator of the Knudsen Compressor. Fig. 6 presents pressure ratios along the centerline of the simulation domain for different connector Knudsen numbers ($Kn_{H/2}$, H= height of the connector section). For a small $Kn_{H/2}$ (eg. 0.11), the pressure increase through the membrane channel could be maintained till the end of the connector section ($p/p_{L,avg}$ ~ 1.24 at x/h =80). As $Kn_{H/2}$ increases, the pressure ratio at the end of the connector section drops significantly. It is evident that the internal flow circulations introduced significant pressure drops through the hot connector section at higher Knudsen numbers, compromising the Knudsen Compressor's performance. The impact of thermally induced internal flows on the performance of Knudsen Compressors is discussed by Han.[51]

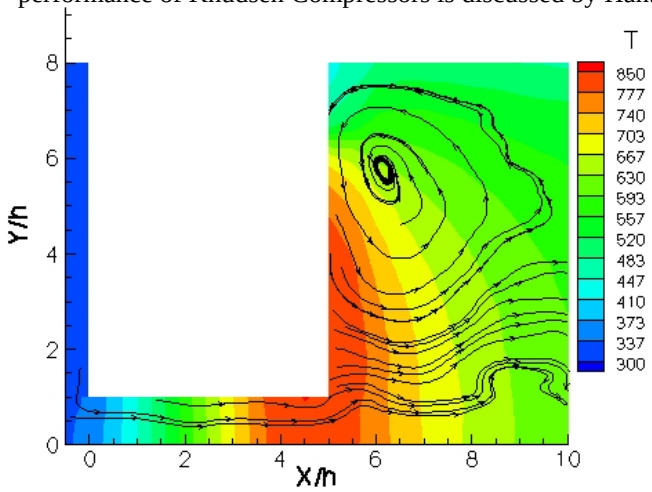

Figure 5 Thermally Induced Internal Flow Circulations

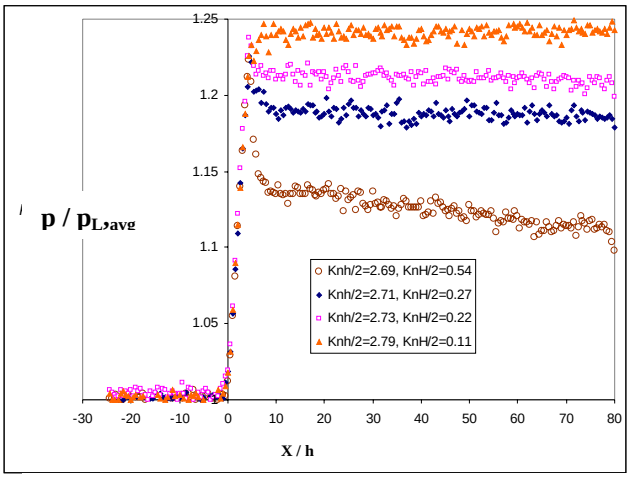

Figure 6 Pressure Ratios along the Centerline of the Simulation Domain

CONTINUOUS TRACE GAS PRE-CONCENTRATOR

The operating theory and the preliminary design of the preconcentrator was based on three separation mechanisms: mass separation, quantum separation, and size separation. The pumping chambers and flow channels of the continuous preconcentrator[52] are illustrated in Fig. 7. The flow channel has a constant height and varying width, while the pumping chambers have constant widths and varying heights. Nanomembranes form the upper and lower surfaces of the concentrator's flow channel. Pumping chambers back each of the nanomembranes. Sampled gas is continuously drawn into the flow channel from the local atmosphere or other source. In order to minimize pumping energy requirements both the flow speed of the sampled gas and its number density remain essentially constant throughout the flow channel. The sampled gas is overwhelmingly a diluent or carrier gas, with trace concentrations (1 to 10^{-3} ppb) of target molecules. It is of interest to enhance the trace concentrations of the target molecules. As the sampled gas travels down the flow channel the generally lighter and smaller diluent gas molecules preferentially escape through the nanomembranes into the pumping chambers. The flow channel has a height of around 100 μm and the flow is well into the continuum flow regime with a pressure of one Earth atmosphere, while the flow through the nanomembranes is in the molecular flow regime. The width of the flow channel is adjusted to account for the loss of carrier gas through the nanomembranes in order to keep the flow speed constant throughout the separation stage. The cross-sectional area of the pumping chambers, perpendicular to the downstream *x* direction in the channel, is adjusted by changing the height of the chambers according to the requirements of continuity. The result is both a constant average flow speed in the *x* direction and an approximately constant diluent gas number density throughout the pumping chambers.

For the analysis of the basic flow field of the preconcentrator, concentrations of the target molecules were assumed to be so small that they have no influence on the gas dynamics in the flow channel. Once the diluent flow field is determined, the target molecules are introduced by linear superposition. The separation membranes were modeled as an array of aligned capillaries with nanometer to subnanometer internal diameters and relatively short lengths. As a consequence of diffusive or mass selection and/or size selection, the membranes inhibit target molecules from passing through the capillaries while allowing the diluent gas to pass more freely. The capillaries will be in the collisionless flow regime up to pressures of one atmosphere. For the preconcentrator to work continuously for long periods, it is most convenient if the target molecules or other gases do not condense in the capillaries due to the phenomenon of pore condensation. Thus, the rejection of these molecules from the capillaries may be important. Theoretically, two rejection phenomena, quantum and size sieving can be considered.[52] In quantum rejection the channel diameters are marginally larger than if the filtering is based on pure size sieving, as in molecular sieve materials. Quantum sieving can be estimated based on the gas-molecule/surface-molecule interactions.[53]

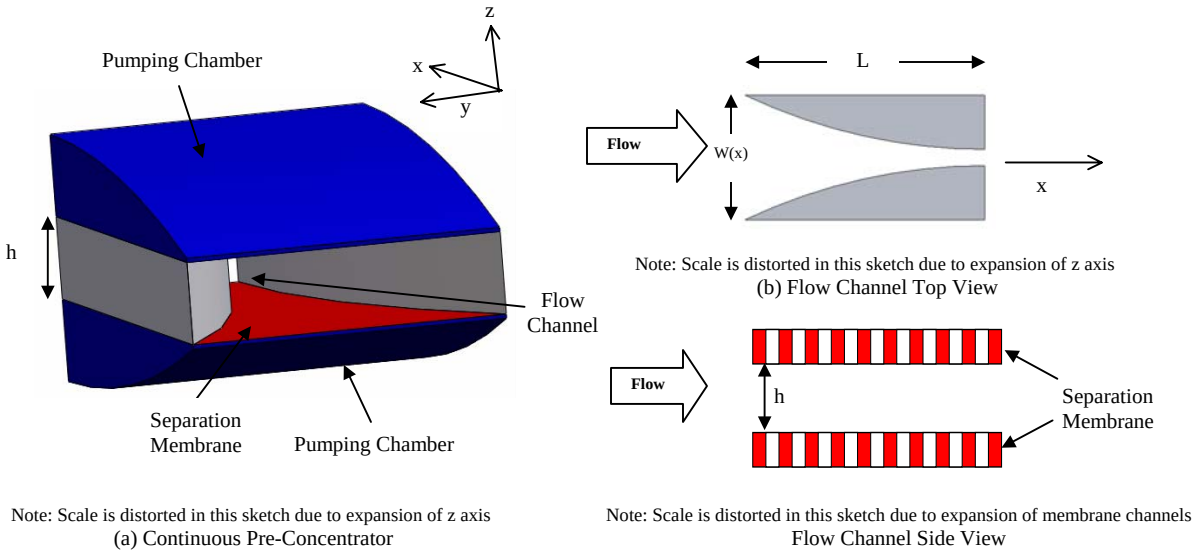

Figure 7 Illustration of the Continuous Trace Gas Preconcentrator

For the preconcentrator application, an initial theoretical analysis[52] has predicted excellent performance if a suitable membrane is employed. Fig. 2 illustrates the concentration of the target molecules at a distance, *x*, from the inlet for a single concentration stage, obtained using the analytic estimates in Ref. 52. The open area fraction for the target molecules, FT, is varied from 0, corresponding to complete physical or quantum filtration of the target molecules, to FA, the same open area fraction as for the diluent molecules. For the latter case the concentration is provided only by the difference in mean thermal speeds of the diluent and target molecules. For these results the diluent gas was assumed to be air and the target gas had an assumed molecular weight of 150. Unlike traditional gaseous diffusion separations, which are notorious users of pumping energy, the approach here is to employ a relatively small pressure ratio of two or less. For the data presented in Fig. 8 the pressure ratio was 0.5, and the flow speed was 2.5 cm/s. At a distance of 1.5 cm it is possible to concentrate the target molecules by a factor of 10 with no size filtration. With complete size filtration the concentration increase is a factor of 100 at a shorter distance.

In order to achieve the performance discussed above, the requirements for the separation membrane can be realized as the following: be thin enough for individual channels to have relatively high transmission probabilities or pumping speeds; have a high open area fraction (preferably > 0.01); and be strong enough to support moderate pressure differences (pressure ratio ~ 2).[52]

Several techniques for assembling arrays of nanometer scale capillary channels with acceptably small length to diameter ratios for use in transmission membranes have been demonstrated.[54,55,56] Martin et al reported the construction of template-synthesized nanotube membranes.[54] Based on commercially available nanoporous membranes as a template, polymer is synthesized by oxidative polymerization of the corresponding monomer within the pores. This may be accomplished either electrochemically or with a chemical oxidation agent. The inner pore diameter of the template-synthesized membrane can be smaller than 3nm and the size and thickness of the

membrane can be easily controlled according to selected templates. However, the fractional open area can barely meet the 0.01 requirement. Unless higher pore density and smaller pore diameter of the templates can be achieved, the template-synthesized membranes would not be able to provide satisfactory results in preconcentrator applications.[52]

Aligned multi-walled carbon nanotube membranes reported by Hinds et al[55] were obtained by filling space between CNTs with a continuous polymer film, the normally closed ends of the CNTs were etched open. The length of the nanotubes within the polymer can be reduced by selective electrochemical oxidation. This makes the membrane thickness flexible. A membrane with 5μm thickness, 7.5 nm inner tube diameter, and with a fractional open area of 0.027 has been demonstrated. The great improvement of the fractional open area from the template-synthesized polymer membrane compared to the multi-walled carbon nanotube membrane assures the initial choice of carbon nanotube membranes as preconcentrator membranes. Also, simulation results[57] have shown that Ar and Ne transport diffusivities are about three orders of magnitude higher in single-walled carbon nanotube membranes than in silicalite membranes with the same thickness.[57] However, experimental validations have not been performed.

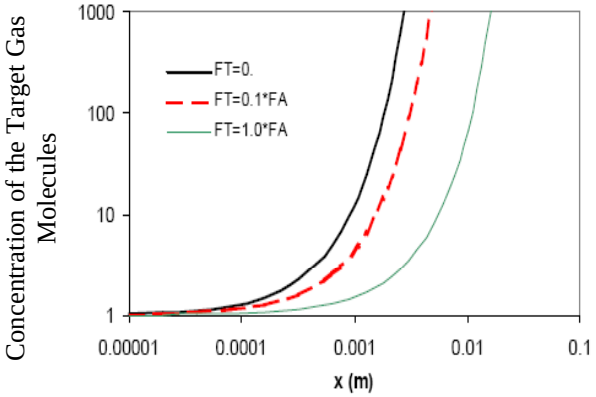

Figure 8 Target Gas Concentration Effectiveness – Flow Speed =2.5cm/s

Another carbon nanotube membrane is the "bed-of nails" membrane made from single-walled carbon nanotubes developed by Smalley et al.[56] Suspended in a fluid, SWNTs can be oriented by applying a magnetic and/or electric field. SWNTs become aligned with their longitudinal axes parallel to the applied field. The aligned SWNTs are removed from the suspension in such a way that they can be assembled while maintaining their alignment. The desirable properties of this membrane are ultrahigh pore density, up to 10^{14}/ cm^2, and a narrow distribution of pore size that is tunable from 0.4 to 3 nm. This method originally presented a membrane with sizes up to 15 μm x 15 μm, thicknesses of 75 nm or less, and with a fractional open area of 0.7. Within one year, a membrane of area more than 1 cm^2 and thickness more than 1 μm was produced.[58] This progress demonstrates the rapid growth of carbon nanotube membrane technology.

Single-walled or multi-walled carbon nanotube membranes are the primary choices for the continuous trace gas preconcentrators due to the large fraction of open area. Currently, fabrication of such carbon nanotube membranes has been initiated.[59] The experimental validation of the continuous trace gas preconcentrators will follow successful creation of a candidate membrane.

Careful studies of candidate membranes, including pumping using an applied temperature difference, will rely on the techniques developed from studies of Knudsen Compressors that have been as discussed above and have been reported in several publications.[14,15,16,44]

SUMMARY

Work at USC on low speed rarefied flows has been outlined. There are a surprising number of widely varying applications where such flows are important.

ACKNOWLEDGMENTS

The work discussed here has been supported by NASA NAG5-10399, AFRL, a University of Southern California Women in Science and Engineering Post-Doctoral Fellowship and the A. B. Freeman Chair's Research Fund.

REFERENCES

[1] E. P. Muntz, Y. Sone, K. Aoki, S. Vargo, M. Young, *J. Vac. Sci. Technol*., **A1**, 214 (2002).
[2] D. C. Wadsworth, E.P. Muntz, *J. Micromechanical Systems*, (1995).
[3] E.P. Muntz, in *Rarefied Gas Dynamics*, edited by R. Brun, R. Carpangue, R. Gatignal, J.-C. Lengrand, Cepduer Edition, Toulence, **1**, 3 (1998)
[4] G.A. Bird, *Molecular Gas Dynamics and the Direct Simulations of Gas Flows*, Oxford University Press (1994).
[5] M.S, Ivanov, G.N, Markelov, S.F. Gimelshein, AIAA Paper 98-2669 (1998)
[6] G. Pham-Van-Diep, D. Erwin, E. P. Muntz, *Scienc*e, **245**, 624 (1989).
[7] A. Alexeenko, S. Gimelshein, E. P. Muntz, A. Ketsdever, *Int. J. Thermal Sciences*, in press. (2006)
[8] D.C Wadsworth, E. P. Muntz, G. Pham-Van-Diep, P. Keeley, in *Rarefied Gas Dynamics*, edited. J. Harvey and G Lord, Oxford University Press, 708 (1995).
[9] G. Pham-Van-Diep, P. Keeley, E. P. Muntz, D. C. Wadsworth, in *Rarefied Gas Dynamics*, edited by J. Harvey and G. Lord, Oxford University Press, 701 (1995).
[10] M. Ota, N. Katawa, in *Rarefied Gas Dynamics*. edited by J. Harvey and G. Lord. Oxford: Oxford University Press, 222 (1995).
[11] T. Soga, Y. Iwayama, H. Oguchi, in *Rarefied Gas Dynamics*. edited by J. Harvey and G. Lord. Oxford: Oxford University Press, 361(1995).
[12] K. Aoki, Y. Sone, N. Masukawa, in *Rarefied Gas Dynamics*. edited by J. Harvey and G. Lord. Oxford: Oxford University Press, 35 (1995).
[13] G. Pham-Van-Diep, P. Keeley, E. P. Muntz, D. P. Weaver, in *Rarefied Gas Dynamic*s, edited by J. Harvey and G. Lord, Oxford University Press, 715 (1995).
[14] S. E. Vargo, Ph.D. Thesis, Los Angeles, CA: University of Southern California (2000).
[15] M. Young, Ph.D. Thesis, Los Angeles, CA: University of Southern California (2004).
[16] Y.-L. Han, Ph.D. Thesis, Los Angeles, CA: University of Southern California (2006).
[17] Y. Sone, Y. Waniguchi, and K. Aoki**,** *Physics of Fluids*, **8**, 2227 (1996)
[18] K. Aoki, Y. Sone, S. Takata, K. Takashashi, and G.A. Bird, in *Rarefied Gas Dynamics*, AIP Conference Proceedings **585**, edited by. T.J. Bartel and M. A. Gallis, Melville, New York, 940 (2001).
[19] Y. Sone, and H. Sugimoto, in *Rarefied Gas Dynamics*, AIP Conference Proceedings **663**, edited. A D Ketsdever and E P Muntz, Melville, New York, 1041 (2003).
[20] H. Sugimoto, and Y. Sone, in *Rarefied Gas Dynamics*, AIP Conference Proceedings **762**, Ed. M Capitelli, Melville, New York, 162, (2005).
[21] W. Crookes, *Proc. Roy. Soc.*, **Ser. A, 23**, 373 (1875).
[22] O. Reynolds, *Phil. Trans. Roy. Soc. London*, **Ser. A, 166**, 725 (1876).
[23] Maxwell, J.C., *Phil. Trans. Roy. Soc. London*, **Ser. A, 170**, 231 (1879).
[24] M. Knudsen, *Ann. Phys.*, **31**, 205 (1910).
[25] M. Knudsen, *Ann. Phys.*, **33**, 1435 (1910).
[26] A. Einstein, *Z. Physik*, **37**, 1 (1924).
[27] H.E. Marsh, L.B. Loeb, *J.O.S.A. & R.S.I*., **11**, 257 (1925)
[28] H.E. Marsh, *J.O.S.A. & R.S.I*., **12**, 135 (1926)
[29] G. Hettner, *Z. Physik*, **27**, 179 (1926).
[30] E. Brueche and W. Littwin, *Z. Physik*, **52**, 318 (1928).
[31] L. Loeb, *Knietic Theory of Gases*, New York (1961).
[32] E. H. Kennard, *Kinetic Theory of Gases*, McGrew Hill, New York, NY (1938).
[33] S. Dushamn, *Scientific Foundations of Vacuum Technique*, John Wiley & Sons, New York, NY (1962).
[34] M.N.Kogan, *Annual Review of Fluid Mechanics*, **5**, 383 (1973).
[35] M.N.Kogan, V.S. Galkin, O.G. Fridlender, *Usp. Fiz. Nauk*., **119**, 111 (1976).
[36] M.N.Kogan, in *Rarefied Gas Dynamics*, edited by Boffi, and Cercignani, B.G.Teubner Stuttgart, 15 (1986).
[37] Y. Sone, Journal de Mécanique théorique et appliquée, **4(1)**, 1 (1985).
[38] Y. Sone, in *Rarefied Gas Dynamics*, edited by Shen, Peking University Press, Beijing, China, 3 (1997).
[39] C. Cercignani, *Slow Rarefied Flows*, Birkhäuser,, Basel, Switzerland (2006).
[40] G.A. Bird, *Molecular Gas Dynamics*, Clarendon Press, Oxford (1976).
[41] A.A. Alexeenko, S.F. Gimelshein, E.P. Muntz, and A.D. Ketsdever, AIAA Paper 2005-963.
[42] A., Alexeenko, S. F., Gimelshein, E.P., Muntz, A. Ketsdever, *Proceedings of the 3rd International Conference on Microchannels and Minichannels.* Toronto, Ontario, Canada: ASME (2005).
[43] A.A. Alexeenko, E.P. Muntz, M. Gallis, J. Torczynski, AIAA Paper, p. 3715 (2006).
[44] Y.-L,. Han, A. A., Alexeenko, M., Young, E. P., Muntz, *Nanoscale and Microscale Thermophysical Engineering* (in press)
[45] D.C Wadsworth, E. P. Muntz, *J. Microelectromechanical Sysytem*, **5 (1)**, 59 (1996).
[46] A. Passion, R.J. Warmock, T.L. Ferrell, T. Thundat, *Physical Review Letters*, **90 (12)**, 124503-1.
[47] C. H. Park, Ph.D. Thesis, Los Angeles, CA: University of Southern California (2006).
[48] G. Benford, J. Benford, *Acta Astronautica*, **56**, 529 (2005).
[49] Y.-L. Han, M. Young, E.P. Muntz, S. Shiflett, in *Rarefied Gas Dynamics*, edited by M. Capitelli, AIP Conference Proceedings **762**, American Institute of Physics, Melville, NY, 162 (2005).
[50] Y.-L. Han, E. P. Muntz, *J. Vac. Sci. Eng.* (2007, in press).
[51] Y.-L. Han, *Proceedings of 25th International Symposium on Rarefied Gas Dynamics* (2006).
[52] E.P. Muntz, M. Young, Y.-L. Han, IMECE 2004-61807, ASME, Anaheim (2004).
[53] J. J. M. Beenakker, V. D. Borman, S. Yu. Krylov, *Chemical Physics Letters*, **232**, 379 (1995).
[54] C. R. Martin, M. Nishizawa, K. Jirage, M. Kang, *J. Phys. Chem. B*, **105**, 1925 (2001).
[55] B. J. Hinds, N. Chopra, T. Rantell, R. Andrews, V. Galavas, L. G. Bachas, *Science*, **203**, 62 (2004).
[56] Y. Wang, S. Da, M. J. Kim, K. F. Kelly, W. Guo, C. Kittrell, R. H. Hauge, R. E. Smalley, *J. AM. Chem. Soc.*, **126**, 9502 (2004).
[57] D.M. Ackerman, A.I. Skoulidas, D. S. Sholl, J. K. Johnson, *Molecular Simulation*, **39 (10-11)**, 677 (2003).
[58] "Making macroscopic assemblies of aligned carbon nanotubes", *NASA Tech Briefs*, March 2005.
[59] Collabration with Prof. C. Zhou, USC, 2006-2007.